

# Shannon invariants: A scalable approach to information decomposition

Aaron J. Gutknecht,<sup>1,\*</sup> Fernando E. Rosas,<sup>2,3,4,5,†</sup> David A. Ehrlich,<sup>1,6</sup>  
Abdullah Makkeh,<sup>1,6</sup> Pedro A. M. Mediano,<sup>7,8</sup> and Michael Wibral<sup>1,6</sup>

<sup>1</sup>*Göttingen Campus Institute for Dynamics of Biological Networks, Georg-August University Göttingen*

<sup>2</sup>*Sussex Centre for Consciousness Science and Sussex AI,*

*Department of Informatics, University of Sussex*

<sup>3</sup>*Center for Psychedelic Research and Centre for Complexity Science,*

*Department of Brain Science, Imperial College London*

<sup>4</sup>*Center for Eudaimonia and Human Flourishing, University of Oxford*

<sup>5</sup>*Principles of Intelligent Behaviour in Biological and Social Systems (PIBBSS)*

<sup>6</sup>*Max Planck Institute for Dynamics and Self-Organization, Göttingen*

<sup>7</sup>*Department of Computing, Imperial College London*

<sup>8</sup>*Division of Psychology and Language Sciences, University College London*

Distributed systems, such as biological and artificial neural networks, process information via complex interactions engaging multiple subsystems, resulting in high-order patterns with distinct properties across scales. Investigating how these systems process information remains challenging due to difficulties in defining appropriate multivariate metrics and ensuring their scalability to large systems. To address these challenges, we introduce a novel framework based on what we call *Shannon invariants* — quantities that capture essential properties of high-order information processing in a way that only depends on the definition of entropy, and can be efficiently calculated for large systems. Our theoretical results demonstrate how Shannon invariants can be used to resolve long-standing ambiguities regarding the interpretation of widely used multivariate information-theoretic measures. Moreover, our practical results reveal distinctive information-processing signatures of various deep learning architectures across layers, which lead to new insights related to how these systems process information and how this is attained throughout training. Overall, our framework resolves fundamental limitations in analysing high-order phenomena and offers broad opportunities for theoretical developments and empirical analyses.

## I. INTRODUCTION

Understanding how information is processed and distributed across systems is a fundamental challenge in multiple scientific domains, from genetics and neuroscience to machine learning and artificial intelligence [1–3]. Advances in our understanding of distributed information phenomena have led to powerful new insights into, for example, the inner workings of natural evolution [4], genetic information flow [5, 6], psychometric interactions [7, 8], cellular automata [9, 10], and polyphonic music [11]. Analyses based on distributed information phenomena have been particularly useful for studying biological [12–18] and artificial [19–22] neural systems, shedding light on the distinct roles of qualitatively different types of information in neural dynamics [23].

The *partial information decomposition* (PID) framework provides a comprehensive theoretical solution to the challenge of understanding distributed information processing by decomposing information carried by multiple source variables about a target into redundant, synergistic, and unique contributions [24–26]. PID has been used, for example, to investigate how artificial neural networks encode and distribute information across multiple nodes

or layers [20, 27], to develop new types of self-organising AI systems that explicitly optimise specific PID-defined objectives [28–30], and to explore how redundancies and synergies complement each other in balancing robustness and flexibility [10, 23, 31].

Unfortunately, despite its promise, PID suffers from important shortcomings related to its operationalisation and scalability. In fact, there are multiple ways to measure redundancy and synergy [24, 32–36], and it is not always straightforward to pick the optimal measure for a specific analysis (for a comprehensive overview and categorization of these measures, see [37]). Moreover, the computational complexity of PID grows super-exponentially with the number of variables involved, rendering the full decomposition computationally infeasible beyond a handful of variables [38, 39]. Together, these limitations seriously hinder the capability of PID to address practical applications.

Here we address these challenges by introducing a novel approach to information decomposition inspired by statistical mechanics. In statistical mechanics, systems with an enormous number of particles are analysed by focusing on global properties — such as their average energy — which can be calculated without knowledge of microscopic details [40, 41]. Similarly, in the context of PID, one deals with a vast number of ‘information atoms’. While it is impractical to measure each information atom individually, we demonstrate that global properties can be determined without needing to resolve the detailed structure of the PID. We introduce two such

\* agutkne@uni-goettingen.de

† f.rosas@sussex.ac.uk

These authors contributed equally to this work.

average properties: the *average degree of redundancy*, which captures the extent to which information can be accessed through multiple variables, and the *average degree of vulnerability*, which reflects how information becomes inaccessible when specific sources are removed.

We illustrate the benefits of these two Shannon invariants in the theoretical and practical domains. On the theoretical side, we show how the degree of redundancy provides a clear explanation of what is being calculated by the ‘redundancy-synergy index’ [42], a well-known metric in the computational neuroscience literature whose interpretation has nevertheless remained elusive [43, 44]. We also show how the degree of vulnerability naturally leads to a novel quantity, which we call ‘dual redundancy-synergy index’. On the practical side, we show how Shannon invariants allow us to analyse deep learning systems, including a feed-forward image classifier and a variational autoencoder. For these systems, our results show that Shannon invariants track distinct representational properties between layers and also distinct learning dynamics, providing useful tools for AI interpretability.

## II. INFORMATION DECOMPOSITION AND SHANNON-INVARIANT QUANTITIES

### A. Shannon-invariance

Let us consider a scenario where  $n$  random variables  $\mathbf{X} = (X_1, \dots, X_n)$ , called *sources*, provide information about a *target* variable  $Y$ . The total information about  $Y$  provided by the  $\mathbf{X}$  can be quantified by Shannon’s mutual information  $I(\mathbf{X}; Y)$  [45]. While this quantity describes *how much* information is provided, it does not explain *in what way* this information is distributed over the various source variables — e.g., if some of this information is redundantly or synergistically contained in multiple components. This second question is addressed by *partial information decomposition* (PID) [24], which states that the total information  $I(\mathbf{X}; Y)$  can be decomposed as

$$I(\mathbf{X}; Y) = \sum_{\alpha \in \mathcal{A}_n} \Pi(\alpha), \quad (1)$$

where each information atom  $\Pi(\alpha)$  quantifies a distinct informational contribution. Here, each  $\alpha$  is a collection of subsets of sources such as  $\{\{1\}, \{2\}\}$ , or  $\{\{1\}, \{2, 3\}\}$ , or simply  $\{\{1\}\}$ . Intuitively, the atom  $\Pi(\alpha)$  quantifies the information about  $Y$  that can be obtained if and only if one knows all the sources in at least one of the subsets in  $\alpha$ . When considering  $n = 2$  sources, there are four such information atoms and Eq. (1) becomes

$$I(X_1, X_2; Y) = \Pi(\{1\}, \{2\}) + \Pi(\{1, 2\}) + \sum_{i=1}^2 \Pi(\{i\}), \quad (2)$$

where the resulting atoms can be described as:

- *Unique information*  $\Pi(\{1\})$  and  $\Pi(\{2\})$  contained in  $X_1$  or  $X_2$ , respectively.
- *Redundant information*  $\Pi(\{1\}\{2\})$  contained in both  $X_1$  and  $X_2$ .
- *Synergistic information*  $\Pi(\{1, 2\})$  contained in  $X_1$  and  $X_2$  jointly, but not contained in either of them individually.

More details about PID can be found in Appendix A.

While calculating individual information atoms  $\Pi(\alpha)$  requires going beyond Shannon information theory [46], certain linear combinations of atoms are determined by classical information theoretic quantities. For example, if  $n = 2$  then the mutual information  $I(X_1; Y)$  can be decomposed as  $I(X_1; Y) = H(X_1) + H(Y) - H(X_1, Y) = \Pi(\{1\}) + \Pi(\{1, 2\})$ , showing that  $\Pi(\{1\}) + \Pi(\{1, 2\})$  does not depend on how  $\Pi(\{1\})$  and  $\Pi(\{1, 2\})$  are measured. Building on this idea, we introduce the notion of *Shannon-invariance* in the next definition.

**Definition 1.** A linear combination of atoms is said to be *Shannon-invariant* if it can be calculated solely from Shannon’s entropies.

A well-known example of a non-trivial Shannon invariant is the difference between redundancy and synergy for  $n = 2$  sources, which can be shown to be given by [24]

$$\Pi(\{1\}, \{2\}) - \Pi(\{1, 2\}) = I(X_1; Y) - I(X_2; Y|X_1) \quad (3)$$

where  $I(X_1; Y) - I(X_2; Y|X_1)$  is known as *interaction information* [47]. This shows that while the value of  $\Pi(\{1\}, \{2\})$  and  $\Pi(\{1, 2\})$  may depend on the way one defines these quantities, their difference does not — it depends only on Shannon’s entropy.

Overall, Shannon-invariant quantities are theoretically attractive, as they establish properties that must be satisfied by any PID. Additionally, Shannon-invariant quantities are particularly useful for practical analyses. In the following, we will introduce two nontrivial Shannon invariants that correspond to distinct perspectives over redundancy and synergy.

### B. Degree of redundancy

When considering only two sources there is just one ‘type’ of redundancy — namely, the one involving both sources, which is captured by the information atom  $\Pi(\{1\}\{2\})$ . However, the concept of redundancy is far richer in analysing systems with more than two sources. For example, when considering  $n = 4$  sources, redundancy can involve information that is contained in two sources (e.g.,  $\Pi(\{1\}\{3\})$ ), three sources (e.g.,  $\Pi(\{1\}\{3\}\{4\})$ ), or all four sources ( $\Pi(\{1\}\{2\}\{3\}\{4\})$ ). More intricate cases arise when an atom involves multiple single sources as well as combinations of sources such as  $\Pi(\{1\}\{2\}\{3, 4\})$ , where information about  $Y$  is

redundantly present in the sources  $X_1, X_2$  and the jointly considered set of sources  $\{X_3, X_4\}$ .

Although information can be redundantly shared between sources in many different ways, a natural way to summarise the *degree of redundancy* of an atom is to count the number of individual sources  $X_i$  through which it can be accessed. This can be formalised as follows:

**Definition 2.** For a given information atom  $\Pi(\alpha)$ , its degree of redundancy  $r(\alpha)$  is given by

$$r(\alpha) := |\{i \in [n] \mid \{i\} \in \alpha\}|. \quad (4)$$

where  $[n] = \{1, \dots, n\}$ .

For example, information atoms such as  $\Pi(\{1, 2\})$  have  $r(\alpha) = 0$  since they cannot be accessed from any individual source;  $\Pi(\{1\}\{2, 3\})$  has  $r(\alpha) = 1$  since it can be accessed from one individual source; and  $\Pi(\{1\}\{2\})$  has  $r(\alpha) = 2$  since it can be accessed from two sources. It can be argued that the information that is ‘genuinely redundant’ consists of atoms with  $r(\alpha) > 1$ , while information atoms with  $r(\alpha) = 0$  are synergistic in the sense that they cannot be accessed from any individual source. The degree of redundancy of the atoms in the case  $n = 3$  sources is illustrated in Figure 1.

Given a set of source variables, one may further ask: what is the *average degree of redundancy* of the information they provide about the target? This quantity is defined as

$$\bar{r} := \sum_{k=0}^n k \sum_{r(\alpha)=k} \frac{\Pi(\alpha)}{I(\mathbf{X}; Y)}. \quad (5)$$

Thus,  $\bar{r}$  represents the *weighted average* of the possible degrees of redundancy  $k$  (ranging from 0 to  $n$ ), where the degree  $k$  is weighted by the fraction of the joint mutual information  $I(\mathbf{X}; Y)$  contributed by information atoms with degree  $k$ . It can be shown that  $\bar{r} \in [0, n]$ , with large values of  $\bar{r}$  characterising redundancy-dominated systems and  $\bar{r} \ll 1$  synergy-dominated systems (see Appendix B). Also, note that  $\bar{r}$  is ill-defined if  $I(\mathbf{X}; Y) = 0$ . Other constructions that estimate an average degree of information atoms have been considered in [27, 48].

Remarkably, while the total information at a given value of  $r(\alpha)$  depends strongly on the specific PID measure used to quantify the atoms, our next result shows that the value of  $\bar{r}$  does not, since it is a Shannon-invariant.

**Proposition 1.** The average degree of redundancy is a Shannon-invariant of the distribution  $p_{\mathbf{X}, Y}$ , and its value can be calculated as

$$\bar{r} = \frac{\sum_{i=1}^n I(X_i : Y)}{I(\mathbf{X}; Y)}. \quad (6)$$

*Proof.* Let us first consider the quantity  $R(\mathbf{X}; Y) := \sum_{i=1}^n I(X_i : Y)$ . All the atoms accounted for by  $R(\mathbf{X}; Y)$  must be accessible from at least one source, and hence

corresponding to the ones with  $r(\alpha) \geq 1$ . Moreover, atoms that appear in multiple mutual information terms are counted multiple times, and the number of mutual information terms an atom appears in is exactly its degree of redundancy  $r(\alpha)$ . Therefore, one can re-write  $R(\mathbf{X}; Y)$  as

$$R(\mathbf{X}; Y) = \sum_{k=1}^n k \sum_{r(\alpha)=k} \Pi(\alpha). \quad (7)$$

The desired result then follows by normalising this by  $I(\mathbf{X}; Y)$ .  $\square$

Note that while  $r(\alpha)$  discriminates between ‘lower-order’ and ‘higher-order’ redundancies — corresponding to values  $r(\alpha) = 2, 3, \dots, n$  — it does not draw such distinctions in the synergy component which corresponds solely to the case  $r(\alpha) = 0$ . Hence,  $r$  looks at redundancies through a finer lens compared to synergies.

### C. Degree of vulnerability

When pondering on the information atoms for  $n = 2$  source variables, one can note that  $\Pi(\{1\}\{2\})$  is the only information that cannot be disrupted by the failure of one source (e.g., if one source suddenly becomes unavailable). Following this intuition, one can describe the *degree of vulnerability* of an atom by identifying the number of sources that are strictly necessary to obtain the information atom — conversely, whose failure would render it inaccessible. For example, the degree of vulnerability of  $\Pi(\{1, 2\}\{1, 3\})$  is one, as there is exactly one source which is strictly necessary to obtain this atom, namely  $X_1$ . In contrast, the degree of vulnerability of  $\Pi(\{1, 2\}\{1, 3\}\{2, 3\})$  is zero because no source is strictly necessary to obtain it. We formalise this notion in the next definition, which captures the number of indices contained in all sets within  $\alpha$  associated with atom  $\Pi(\alpha)$ .

**Definition 3.** For a given information atom  $\Pi(\alpha)$ , its degree of vulnerability  $v(\alpha)$  is given by

$$v(\alpha) := |\{i \in [n] \mid \forall \mathbf{a} \in \alpha : i \in \mathbf{a}\}|. \quad (8)$$

where  $[n] = \{1, \dots, n\}$ .

The name ‘degree of vulnerability’ reflects the fact that  $\Pi(\alpha)$  captures the susceptibility of  $\Pi(\alpha)$  to information loss when individual sources become unavailable. Effectively, the more sources  $\Pi(\alpha)$  critically depends on, the more vulnerable it is. The information atoms with  $v(\alpha) = 0$  can be called *robust* since they do not depend on any particular source. The classification of atoms for  $n = 3$  sources based on their vulnerability is illustrated in Figure 1.

As with the degree of redundancy, one can define the *average degree of vulnerability* as

$$\bar{v} := \sum_{j=0}^n j \sum_{v(\alpha)=j} \frac{\Pi(\alpha)}{I(\mathbf{X}; Y)}. \quad (9)$$

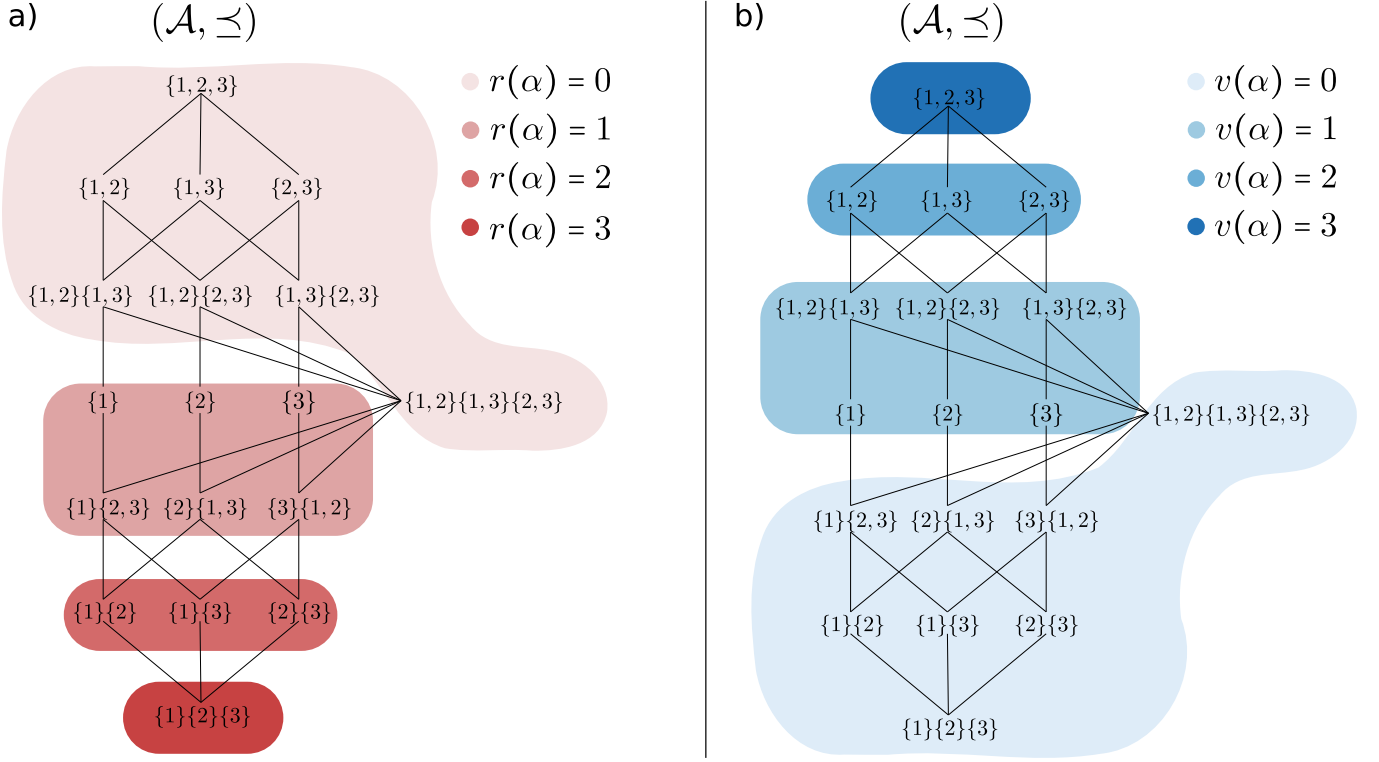


FIG. 1. Illustration for  $n = 3$  of the grouping of atoms in terms of their a) degree of redundancy, and b), degree of vulnerability.

It can be shown that  $\bar{v} \in [0, n]$ , with  $\bar{v} \ll 1$  characterising robust systems and large values of  $\bar{v}$  characterising highly vulnerable ones (see Appendix B). Our next result shows that  $\bar{v}$  is a Shannon-invariant property of the joint distribution of the source and target variables.

**Proposition 2.** *The average degree of vulnerability is a Shannon-invariant of the distribution  $p_{\mathbf{X}, Y}$ , which can be calculated as*

$$\bar{v} = \frac{\sum_{j=1}^n I(X_j; Y | \mathbf{X}_{-j})}{I(\mathbf{X}; Y)}. \quad (10)$$

where  $\mathbf{X}_{-j}$  denotes the collection of all sources except the  $j$ -th source.

*Proof.* Consider the quantity  $V(\mathbf{X}; Y) := \sum_{j=1}^n I(X_j; Y | \mathbf{X}_{-j})$ . The atoms accounted for by  $V(\mathbf{X}; Y)$  are exactly the ones with  $v(\alpha) \geq 1$ . This is because the conditional mutual information  $I(X_j; Y | \mathbf{X}_{-j})$  is the information we obtain from  $X_j$  even if we already know all other sources. But then all such information must critically depend on  $X_j$  and hence has at least  $v(\alpha) = 1$ . Generally, if an atom has  $v(\alpha) = j$ , i.e. it critically depends on  $j$  sources, then it will appear in  $j$  conditional mutual information terms and is hence counted  $j$  times in  $V(\mathbf{X}; Y)$ . This includes the special case of  $v(\alpha) = 0$ : if an atom does not critically depend on any information source, then it does not appear in any CMI. If it did, it *would* critically depend on some

source since knowing all other sources was apparently not enough to obtain it. This implies that

$$V(\mathbf{X}; Y) = \sum_{j=0}^n j \sum_{v(\alpha)=j} \Pi(\alpha). \quad (11)$$

Finally, the desired result then follows by normalising this by  $I(\mathbf{X}; Y)$ .  $\square$

Note that  $v(\alpha)$  distinguishes between lower-order and higher-order vulnerabilities — corresponding to values  $v(\alpha) = 1, 2, \dots, n$  — whereas the robustness is included without further distinction in the case  $v(\alpha) = 0$ . Thus,  $v$  looks at vulnerability through a finer lens compared to robustness.

#### D. Different views on redundancies and synergies

The degrees of redundancy and vulnerability introduced above reveal two distinct ways to think about redundancy and synergy:

- *Source-level redundancy and synergy:*  $r$  distinguishes atoms in terms of how many individual sources can provide a given information atom. Thus,  $r > 1$  takes place when the information can be provided redundantly by more than one single source, and  $r = 0$  when it cannot and is hence synergistic with respect to the sources.



- *Robustness and vulnerability*:  $v$  distinguishes information atoms based on how easy or hard they are to disrupt. Robustness ( $v = 0$ ) reflects that the information is redundant in a way that ensures it remains accessible even if any individual source is lost. However, this form of redundancy does not necessarily mean that the information is accessible through multiple *individual* sources (e.g.,  $\Pi(\{1, 2\}\{1, 3\}\{2, 3\})$  is robust). On the other hand, vulnerability (for  $v > 1$ ) is a form of synergy, as an atom that critically depends on more than one source cannot be obtained from any individual source alone.

Interestingly, there are logical relationships between the two different notions of redundancy and synergy.

- Source-level redundancy is stronger than robustness, i.e. the information atoms with  $r(\alpha) > 1$  are a subset of the atoms with  $v(\alpha) = 0$ .
- Vulnerability (of degree larger one) is stronger than source-level synergy, i.e. the atoms with  $v(\alpha) > 1$  are a subset of atoms with  $r(\alpha) = 0$ .

For quantifying the total information at a given degree of vulnerability, we define the  $k$ -*vulnerable information* as

$$I_v^{(k)}(\mathbf{X}; Y) := \sum_{v(\alpha)=k} \Pi(\alpha), \quad (12)$$

representing the total information that critically depends on exactly  $k$  sources. For  $k = 0$ , this is the total *robust information*. Similarly, we define the  $k$ -*redundant information* as

$$I_r^{(k)}(\mathbf{X}; Y) := \sum_{r(\alpha)=k} \Pi(\alpha), \quad (13)$$

representing the total information accessible through exactly  $k$  sources. For  $k = 0$ , this is the *source-level synergy*.

Assuming non-negative atoms, the following inequalities are implied by the logical relationships between the concepts:

$$I_v^{(0)}(\mathbf{X}; Y) \geq \sum_{k=2}^n I_r^{(k)}(\mathbf{X}; Y) \quad (14)$$

$$I_r^{(0)}(\mathbf{X}; Y) \geq \sum_{k=2}^n I_v^{(k)}(\mathbf{X}; Y). \quad (15)$$

The relationships between the different notions of redundancy and synergy are summarized in Table I. The two notions coincide only for the case of  $n = 2$  source variables, with source redundancy and robustness corresponding to the atom  $\Pi(\{1\}\{2\})$ , and source synergy and vulnerability of degree larger one corresponding to the atom  $\Pi(\{1, 2\})$ .

Before concluding, it is worth noting a subtle asymmetry in the interpretation of  $r(\alpha)$  and  $v(\alpha)$ , which is

TABLE I. Weaker and stronger notions of redundancy and synergy.

	Redundancy	Synergy
Weaker ( $k = 0$ )	$I_v^{(0)}(\mathbf{X}; Y)$ (robustness)	$I_r^{(0)}(\mathbf{X}; Y)$ (source-level syn.)
Stronger ( $k > 1$ )	$I_r^{(k>1)}(\mathbf{X}; Y)$ (source-level red.)	$I_v^{(k>1)}(\mathbf{X}; Y)$ (vulnerability)

rooted in how the words ‘redundancy’ and ‘vulnerability’ are used in ordinary language. For redundancy, only  $r > 1$  corresponds to genuine redundancy (for example, if your network administrator reassured you, “Don’t worry about your data; I’ve stored it redundantly,” you would expect it to be backed up on *more* than one independent hard drive). For vulnerability, however,  $v = 1$  already signals vulnerability (e.g. if the structural integrity of a house depends on a single critical screw—such a house is undoubtedly vulnerable; there is no need for two critical screws to classify it as such).

### III. COMPARING REDUNDANCY AND SYNERGY

Here we highlight theoretical advances related to the framework of Shannon invariants. In particular, we show how the degree of redundancy and vulnerability let us interpret existent high-order metrics and suggest new ones.

#### A. Understanding the Redundancy-Synergy index

We start by presenting how the analysis related to the degree of redundancy leads to a rigorous interpretation of the *redundancy-synergy index* (RSI) [49], which is one of the most widely considered metrics to assess the balance between redundant and synergistic information [43, 50–56]. The RSI is defined as

$$\text{RSI}(\mathbf{X}; Y) := \sum_{i=1}^n I(X_i; Y) - I(\mathbf{X}; Y). \quad (16)$$

Its underlying intuition is that if the information is predominantly redundant, the sum of mutual information contributions  $I(X_i; Y)$  should be much larger than the joint mutual information  $I(\mathbf{X}; Y)$ , whereas the latter should be larger than the former if the information is predominantly synergistic. Thus, positive values of the RSI are interpreted as indicating a dominance of redundancy, and negative values indicating a dominance of synergy.

The case of  $n = 2$  predictors had already been used earlier as an indicator of synergy vs redundancy by [50] and even earlier by [51], and the latter considered the ratio of the sum over the total mutual information (i.e.  $\bar{r}$ ) for  $n = 2$ .

The intuitions developed in those early works can be neatly formalised via PID. In effect, by replacing each

mutual information by its corresponding PID atoms, a direct calculation shows that

$$\text{RSI}(X_1, X_2; Y) = \Pi(\{1\}\{2\}) - \Pi(\{1, 2\}), \quad (17)$$

confirming that the RSI for  $n = 2$  predictors captures the difference between redundancy and synergy. From this analysis, it is natural to wonder whether this clear-cut picture generalises for more source variables. Does the RSI for  $n > 2$  still represent the difference between redundancies minus synergies of some sort?

Our next result answers this question by providing a general decomposition of the RSI for any number of source variables using the notions of source-level redundancy and source-level synergy (see Table I).

**Proposition 3.**

$$\text{RSI}(\mathbf{X}; Y) = \sum_{k=2}^n (k-1) I_r^{(k)}(\mathbf{X}; Y) - I_r^{(0)}(\mathbf{X}; Y). \quad (18)$$

*Proof.* By combining Proposition 1 with the fact that

$$I(\mathbf{X}; Y) = \sum_{\alpha \in \mathcal{A}_n} \Pi(\alpha) = \sum_{k=0}^n \sum_{r(\alpha)=k} \Pi(\alpha), \quad (19)$$

one finds that

$$\begin{aligned} \text{RSI}(\mathbf{X}; Y) &= R(\mathbf{X}; Y) - I(\mathbf{X}; Y) \\ &= \sum_{k=0}^n (k-1) \sum_{r(\alpha)=k} \Pi(\alpha) \\ &= \sum_{k=2}^n (k-1) \sum_{r(\alpha)=k} \Pi(\alpha) - \sum_{r(\alpha)=0} \Pi(\alpha), \end{aligned}$$

which gives the desired result.  $\square$

This result shows that the RSI does capture *source-level redundancy* minus *source-level synergy* for any number of source variables. Hence, assuming non-negativity of the information atoms (a property satisfied by some but not all PID approaches),  $\text{RSI} > 0$  implies there must be at least some source-level redundant information, and  $\text{RSI} < 0$  that there must be some source-level synergistic information.

That being said, it is important to notice that if  $n \geq 3$  then there is an asymmetry in how redundancy and synergy are treated: the redundant component involves a weighting, where higher-order redundancies are counted more often than lower-order ones. Specifically, if an information atom is accessible via  $k$  individual sources then it is counted  $k-1$  times, while no such weighting appears in the synergy component. For example, when considering  $n = 3$  predictors, then Eq. (20) states that the RSI can be decomposed as

$$\begin{aligned} \text{RSI}(X_1, X_2, X_3 : Y) &= 2\Pi(\{1\}\{2\}\{3\}) + \Pi(\{1\}\{2\}) \\ &\quad + \Pi(\{1\}\{3\}) + \Pi(\{2\}\{3\}) \end{aligned}$$

$$- I_r^{(0)}(X_1, X_2, X_3 : Y). \quad (20)$$

This asymmetric weighting could give the impression that a rigorous interpretation of the values of the RSI is not straightforward. However, a natural interpretation can be built in terms of the degree of redundancy, as shown by our next corollary.

**Corollary 1.** *The RSI and the average degree of redundancy  $\bar{r}$  are related via*

$$\text{RSI}(\mathbf{X}; Y) = (\bar{r} - 1)I(\mathbf{X}; Y). \quad (21)$$

This result shows that  $\text{RSI} < 0$  if and only if  $\bar{r} < 1$ , implying that a nonzero amount of source-level synergy must be present (assuming non-negative atoms). In contrast,  $\text{RSI} > 0$  takes place if and only if  $\bar{r} > 1$ , implying that some information must be source-level redundant, meaning it can be retrieved from more than one source (again assuming non-negative atoms). Finally, while  $\bar{r}$  is an entirely relative measure, the RSI accounts for the absolute amount of information contained in the sources about the target by multiplying  $(\bar{r} - 1)$  by the total mutual information  $I(\mathbf{X}; Y)$ , thereby providing an ‘effect size’ to quantify the magnitude of these effects.

## B. Dual Redundancy-Synergy Index

The previous section presented how the RSI compares redundancy and synergy at the source-level. Interestingly, building upon the view put forward in Section II D, one may also consider such a comparison in terms of robustness and vulnerability. This suggests the introduction of a *dual redundancy-synergy index* (DRSI), which — constructed in analogy to Proposition 3 — can be defined as

$$\text{DRSI}(\mathbf{X}; Y) := I_v^{(0)}(\mathbf{X}; Y) - \sum_{k=2}^n (k-1) I_v^{(k)}(\mathbf{X}; Y). \quad (22)$$

Above, we have replaced the redundancy components with robustness, and the source-level synergies with vulnerabilities of degree larger than one. Hence,  $\text{DRSI} > 0$  implies (assuming non-negative atoms) there must be at least some robust information, and  $\text{DRSI} < 0$  that there must be some vulnerable information of degree larger one.

One important consequence of the definition of the DRSI is that now the synergistic component involves a weighting where higher-order vulnerabilities are counted more often than lower-order ones. In particular, if an atom has  $v(\alpha) = k$  it is counted  $k-1$  times. The redundant component by contrast involves no such weighting in the DRSI. For example, when considering  $n = 3$  sources then Eq. (22) becomes

$$\text{DRSI}(X_1, X_2, X_3 : Y) = I_v^{(0)}(X_1, X_2, X_3 : Y) -$$

$$2\Pi(\{\{1, 2, 3\}\}) - \Pi(\{\{1, 2\}\}) \\ - \Pi(\{\{1, 3\}\}) - \Pi(\{\{2, 3\}\}). \quad (23)$$

Our next result shows that, just as the RSI, the DRSI is a Shannon invariant of the distribution  $p_{\mathbf{X}, Y}$ .

**Proposition 4.** *The DRSI is a Shannon invariant, and can be expressed as*

$$\text{DRSI}(\mathbf{X}; Y) = I(\mathbf{X}; Y) - \sum_{j=1}^n I(X_j; Y | \mathbf{X}_{-j}). \quad (24)$$

where  $\mathbf{X}_{-j}$  denotes the collection of all sources except the  $j$ -th source.

*Proof.* Starting from the definition of the DRSI we add all atoms with  $v(\alpha) \geq 1$  to each term:

$$\begin{aligned} \text{DRSI}(\mathbf{X}; Y) &= \left( I_v^{(0)}(\mathbf{X}; Y) + \sum_{k=1}^n I_v^k(\mathbf{X}; Y) \right) \\ &\quad - \left( \sum_{k=2}^n (k-1) I_v^{(k)}(\mathbf{X}; Y) + \sum_{k=1}^n I_v^k(\mathbf{X}; Y) \right) \\ &= I(\mathbf{X}; Y) - \sum_{k=1}^n k I_v^{(k)}(\mathbf{X}; Y) \\ &= I(\mathbf{X}; Y) - \sum_{j=1}^n I(X_j; Y | \mathbf{X}_{-j}). \end{aligned}$$

Where the second equality follows because the robustness consists of all atoms with  $v(\alpha) = 0$ , and hence, the first term equals the joint mutual information. In the second term the count of each atom is increased by one including those with  $v(\alpha) = 1$  which were not counted at all before and are now counted once. The third equality follows by the argument given in the proof of Proposition 2 and the definition of  $I_v^{(k)}$ .  $\square$

Similar to how the RSI is related to the average degree of redundancy, a natural interpretation of the DRSI can be built by relating it with the average degree of vulnerability in the following way:

**Corollary 2.** *The DRSI and the average degree of vulnerability  $\bar{v}$  are related via*

$$\text{DRSI}(\mathbf{X}; Y) = (1 - \bar{v}) I(\mathbf{X}; Y). \quad (25)$$

It follows immediately that  $\text{DRSI}(\mathbf{X}; Y) < 0$  if and only if  $\bar{v} > 1$ . Analogous to the RSI, multiplying  $(\bar{v} - 1)$  by the total mutual information  $I(\mathbf{X}; Y)$  provides an effect size that quantifies the magnitude of these effects.

In summary, the RSI and the DRSI are two Shannon invariants that quantify the balance between redundancy and synergy within a set of source variables about a target variable, yet they differ in (i) how redundancy and synergy are interpreted and (ii) which of them is emphasized more strongly. The RSI captures the balance

in terms of source-level redundancy and source-level synergy, emphasising redundant contributions by attributing a higher weight to higher-order redundancies. In contrast, the DRSI captures this balance through robustness and vulnerability, emphasising vulnerable contributions by assigning a higher weight to higher-order vulnerabilities.

#### IV. CALCULATING SHANNON INVARIANTS OF DEEP LEARNING SYSTEMS

Here we show how the concepts of the degree of redundancy and vulnerability can be employed to analyse deep learning systems, shedding new light into how feed-forward classifiers and convolutional autoencoders process information among their neural units.

##### A. Background and estimation

The layers of feed-forward neural networks can be interpreted as successive ‘channels’ that re-encode relevant information to make it extractable for the output layer while removing task-irrelevant elements from the inputs. Following this line of reasoning, one can apply information decomposition to the network’s activation patterns in order to obtain insights on how information about the target — e.g., the classification label or the input of an autoencoder — is encoded by the neural units, how this encoding changes among successive hidden layers, and how it develops throughout training.

Despite its promise, early attempts of using information theory in the study of neural networks have revealed potential pitfalls in this approach. Since classical neural networks work with continuous activation values and are deterministic, they define an injective map from the inputs to their hidden layer activations. Neural networks thus have (at least in theory) an infinite channel capacity, precluding standard information-theoretic analyses [57–59]. Attempts to measure information-theoretic quantities in such settings by binning values or employing continuous mutual information estimators thus do not yield meaningful information-theoretic indicators, but can at most be reinterpreted as measures for geometric clustering depending on the estimation scheme [59]. These shortcomings can be remedied by instead analysing settings that break the network’s injectivity, for example by adding Gaussian noise to the activations [58], or by quantising the activations while training and evaluating [27].

The above considerations are concerned with the well-definedness of information theoretic quantities in neural network analysis. After resolving these theoretical issues, we still face the practical challenge of estimation from finite data samples. Here, it is crucial to distinguish clearly between training and test contexts. The test dataset is typically viewed as a finite sample drawn from a potentially infinite underlying data-generating process,

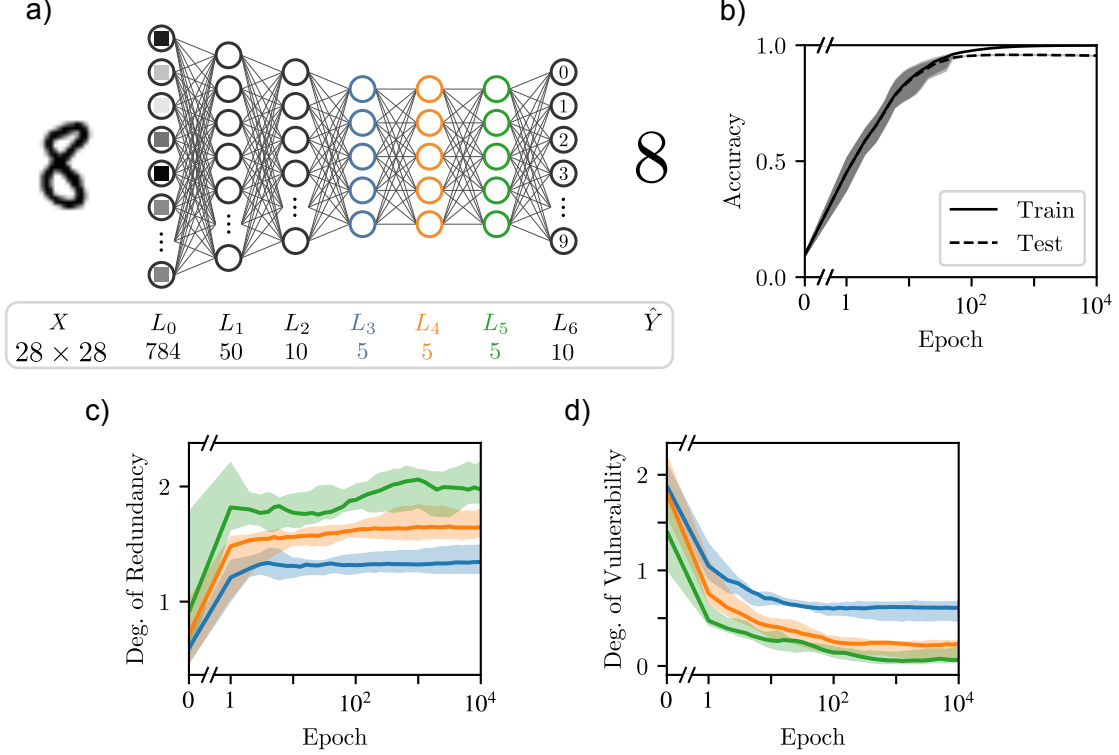


FIG. 2. **In a deep classification network, the degree of redundancy of the layer’s activity about the label increases throughout the hidden layers while the degree of vulnerability decreases throughout the hidden layers and over training.** a) The architecture of the MNIST classification network comprises five fully-connected hidden layers with activation values quantized to eight levels, three of which have the same size of 5 neurons. b) After  $10^4$  training epochs, the classifier reaches an average train set accuracy of 99.89(3)% and a test set accuracy of 95.5(3)%. In all plots, lines represent the median, shaded regions the maximum and minimum of 10 runs with random weight initializations. c), d) Degree of redundancy and degree of vulnerability computed on the training set for the three equal-sized hidden layers.

making it necessary to statistically estimate information-theoretic quantities. In contrast, our approach is to carry out information-theoretic analyses exclusively on the training set, treating it as the complete population with each element assigned equal probability. This allows us to directly *calculate* information-theoretic quantities, bypassing the need for estimation. The scientific question we address with this approach shifts from how the network encodes an unknown, out-of-sample distribution to how it learns to encode this particular training dataset.

The following subsections present analyses of two different deep neural networks: a feed-forward image classifier and a variational autoencoder. Building on the above considerations, we consider those networks with activation values being stochastically discretised to eight levels. From these discretised activations, we construct the full probability mass function of activations invoked by the training set, from which the corresponding information-theoretic quantities are computed. Details of these procedures are presented in Appendix C.

## B. Feedforward MNIST Classification

For our first case study, we trained a small fully-connected quantised feed-forward network to solve the classic *MNIST* handwritten digit classification task [60]. The architecture has been chosen with three hidden layers of the same size to allow an analysis of the information-theoretic measures throughout the layers and over training (see Figure 2.a, cf. [27]). The networks have been trained for  $10^4$  epochs, reaching a test set accuracy of 95.5(3) % (see Figure 2.b).

Our results show that the degree of redundancy of the neuron’s activations with respect to the true classification label increases sharply during the first epoch of training, and then mostly stabilizes with only small increases afterwards in layers  $L_3$  and  $L_4$ . Interestingly, layer  $L_5$  exhibits the same initial increase, but displays a continued increase during later stages of training.

In contrast, the degree of vulnerability decreases over training for all layers, and is also smaller for later layers. Please note that there is no direct mathematical reason for the degree of vulnerability to display the opposite



effect than the degree of redundancy, and hence this non-trivial signature should be regarded as a signature of how feed-forward deep learning systems process information.

The reason why redundancy increases with depth while vulnerability decreases may be attributable to combinatorial considerations — because of the data processing inequality, the amount of information about the input can only decrease over layers. This frees more capacity of the network to encode the remaining relevant information more redundantly, which is reflected in both the degree of redundancy and vulnerability. We conjecture that more redundant encodings may be preferable for the network, as they could lead to representations that are more robust to small input variations and thereby support better generalization.

### C. Face Autoencoder

To further showcase the versatility of our framework, we used the degree of redundancy and vulnerability to investigate how a quantized convolutional autoencoder processes information. For this purpose, we employed a standard convolutional autoencoder architecture with three convolutional encoding layers, a fully connected bottleneck layer of varying size  $n_b$ , and three convolutional decoder layers (see Figure 3.a). This system was trained to reconstitute face images, being trained with the *Labelled Faces in the Wild* dataset [61]. For  $n_b = 128$ , the loss converges after  $10^3$  training epochs and achieves a faithful reconstruction of the original figures (see Figure 3.b).

Results for a bottleneck of  $n_b = 128$  units show that the degree of redundancy in all layers except the first encoder layer quickly increase within the first training epoch, and remain mostly constant afterwards (see Figure 3.c). After the first epoch, the decoder layers exhibit a higher degree of redundancy than the size-matched encoder layers. As with the successive size-matched layers in the MNIST example, this result may be attributable to the fact that the decoder layers encode less overall information, leaving more capacity for the remaining information to be encoded redundantly.

For significantly smaller bottleneck sizes of  $n_b = 12$  to  $n_b = 20$  units, the degree of redundancy in the bottleneck layer converges more slowly than in the case of  $n_b = 128$  (see Figure 3.d). Furthermore, a clear ordering is shown with smaller bottleneck sizes, resulting in a smaller degree of redundancy. This, again, is likely attributable to the ratio between the relevant information the network tries to learn and the channel capacity of the bottleneck layer.

On the other hand, results show that the degree of vulnerability initially increases sharply to approximately 1, and then converges to much lower values all within the first training epoch (see Figure 3.e). This sharp increase, which coincides with a drop in the degree of redundancy, can be attributed to an overall small mutual information

during this brief training period. In effect, with the total mutual information dropping below one bit for some runs, the remaining information may be provided by single neurons that deviate from being constant for some samples, giving rise to an encoding with a degree of synergy and vulnerability of one. Nevertheless, the small values the degree of vulnerability converge to still show an ordering with the largest bottleneck having the lowest vulnerability in later epochs.

## V. DISCUSSION

In this paper we introduced a novel approach for studying higher-order information structure using Shannon invariants. This method circumvents operationalisation and scalability issues of information decomposition by focusing on averages that depend solely on Shannon entropy. By addressing these key limitations, this framework opens the door to a wide range of practical data analyses. The results presented here highlight both the theoretical and practical advantages of this approach, as discussed next.

The formalism developed here reveals that redundancy and synergy can be conceptualized in two complementary ways. First, at the source level, redundancy refers to information that is redundantly accessible from more than one individual source, while synergy describes information that cannot be obtained from any single source. Second, redundancy and synergy can be framed in terms of robustness and vulnerability: robustness represents information that remains accessible even if any individual source is lost, implying that it is redundantly contained within the system though not necessarily in multiple individual sources. Vulnerability, in contrast, captures information that critically depends on at least two specific sources, thus making it synergistic but in a stronger sense than source-level synergy. These different conceptualizations highlight the richness of redundancy and synergy in multivariate systems.

Building on these ideas, we introduced two quantities that position a system on a redundancy-synergy scale, reflecting these two distinct ways of conceptualizing these phenomena. The average degree of redundancy captures the average number of sources redundantly providing information, while the average degree of vulnerability represents the average number of sources on which information critically depends. Crucially, both measures are Shannon invariants, relying solely on the Shannon entropies of the system. This eliminates the need to compute individual information atoms or to adopt a specific definition for them. Furthermore, the computational complexity is efficient, as the number of entropies required scales linearly with the number of source variables.

Additionally, the presented approach reveals new insights into the RSI, a well-known information-theoretic metric whose interpretation has remained elusive, and introduces the novel DRSI. We demonstrated that the RSI

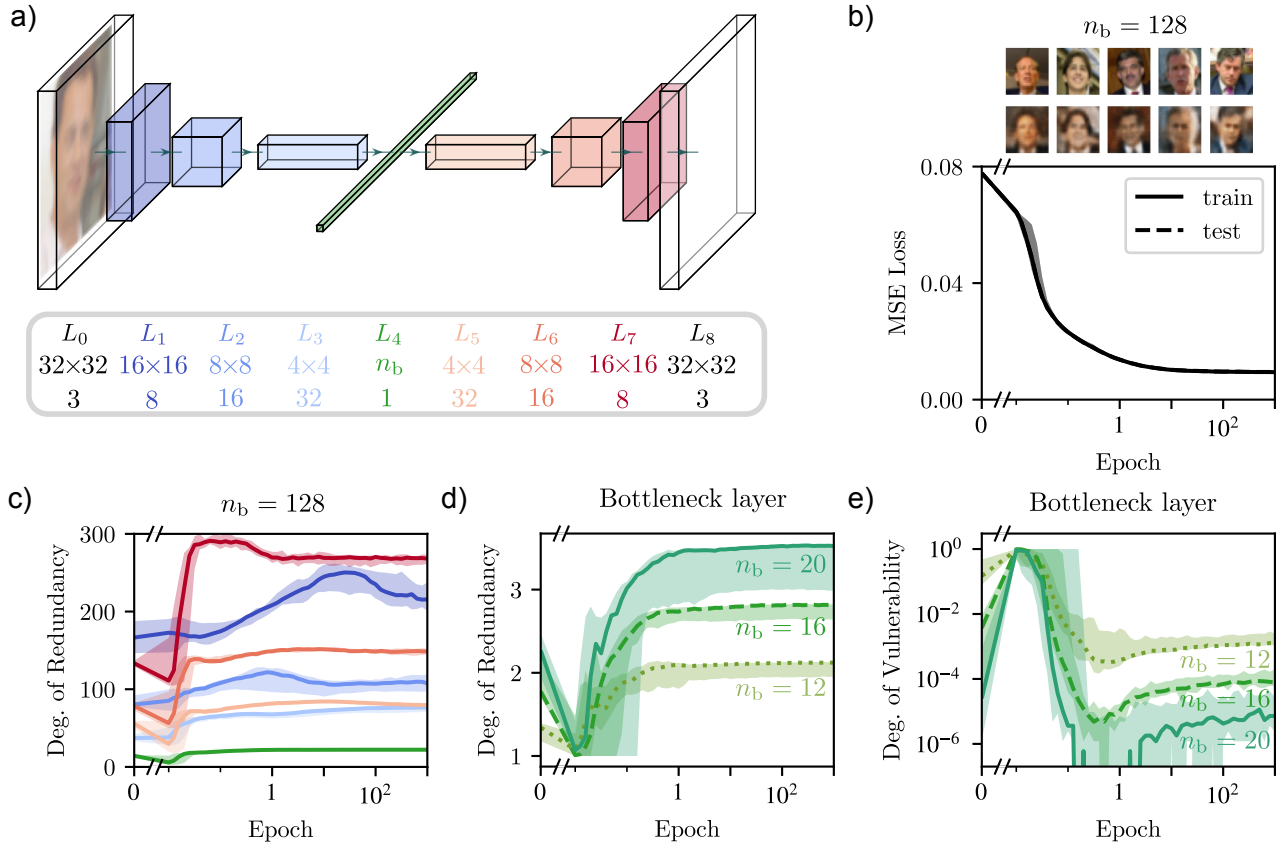


FIG. 3. In a convolutional autoencoder, the degree of redundancy about the input is larger in decoder layers than in the size-matched encoder layers. Furthermore, the degree of redundancy increases with bottleneck size while the degree of vulnerability decreases. a) The architecture of the face image autoencoder comprises a three-layer convolutional encoder, a fully-connected bottleneck layers with varying number of neurons  $n_b$  and a three-layer convolutional decoder. Numbers below the layers reflect the size of the activation matrices as well as the number of channels. b) For a bottleneck size of  $n_b = 128$ , the mean square error loss on the test set converges to  $9.5(1) \times 10^{-3}$  after  $10^3$  epochs. Five original images (upper row) and their reconstruction (lower row) are shown for the converged networks. In all plots, lines represent the median, shaded regions the maximum and minimum of 10 runs with random weight initializations. c) Degree of redundancy computed on the training set, all activations from all convolutional filters have been treated as individual source variables. The degree of vulnerability (not shown) is equal to zero up to numerical error for all layers for a bottleneck layer of width  $n_b = 128$ . d), e) Degree of redundancy and degree of vulnerability of the bottleneck layer for varying small bottleneck sizes  $n_b$ . The inset in E shows an enlarged view of the degree of vulnerability.

is closely related to the average degree of redundancy, while the newly introduced DRSI is connected to the average degree of vulnerability, providing a principled approach to interpret their outcomes. Both metrics quantify the balance between redundancy and synergy, with the RSI doing so in terms of source-level redundancy and synergy, and the DRSI in terms of robustness and vulnerability. Importantly, both metrics treat redundancy and synergy asymmetrically: the RSI places greater emphasis on redundancy, while the DRSI prioritizes synergy.

We demonstrated the practical capabilities of the proposed framework by presenting various analyses of deep learning systems, including feed-forward neural networks and convolutional autoencoders. In the feedforward classifier network, we observe that the degree of redundancy increases over training and throughout successive

equally-sized hidden layers, while the degree of vulnerability displays the opposite behaviour. In the autoencoder network, the degree of redundancy is linked to the bottleneck size, while the vulnerability again shows the inverse trend. These results suggest a general relationship between the amount of information in a layer and how it is encoded: when little information is encoded in a large layer, the encoding tends to be more redundant, while it becomes more vulnerable the closer to capacity the information transfer becomes.

Overall, the framework introduced in this paper addresses the key limitations of information decomposition and brings important theoretical and practical advantages, opening the way to new information decomposition analyses when a full decomposition is unfeasible. Future work may investigate the landscape of possible Shannon

invariants, which may bring new insights into the possible ways of conceptualising synergy and redundancy. Also, future work may develop techniques to improve the estimation of Shannon invariants in large-scale systems, using novel algorithmic approaches [62], de-biasing methods [63] or null models [64].

## ACKNOWLEDGEMENTS

We thank Andreas Schneider for valuable discussions related to this work. The work of F.R. has been supported by the UK ARIA Safeguarded AI programme and by the PIBBSS Affiliateship programme. A.G., D.E., A.M., and M.W. are employed at the Göttingen Campus Institute for Dynamics of Biological Networks (CIDBN) funded by the Volkswagen Stiftung.

## Appendix A: Partial Information Decomposition

Let us consider a scenario where  $n$  random variables  $X_1, \dots, X_n$  provide information about a variable  $Y$ . In addition, let  $[n] = \{1, \dots, n\}$  denote the index set of source variables. The total information about a *target* variable  $Y$  given by the *source* variables  $\mathbf{X} := (X_1, \dots, X_n)$  can be quantified by Shannon’s mutual information [45], which describes the average reduction of uncertainty regarding the value of  $Y$  upon observing  $\mathbf{X}$ :

$$I(X_1, \dots, X_n : Y) = H(Y) - H(Y|\mathbf{X}). \quad (\text{A1})$$

Above, the uncertainty about  $Y$  is quantified by the Shannon entropy  $H(Y)$ , and the conditional uncertainty about  $Y$  given  $\mathbf{X}$  is quantified by the conditional Shannon entropy  $H(Y|\mathbf{X})$ .

A natural question that arises in this setting is *how the information about the target  $Y$  is distributed over the different components of the source  $\mathbf{X}$* . Is some of this information uniquely delivered by a particular component  $X_i$ ? Or perhaps some of it redundantly contained in multiple components? Or some of it may only be available when accessing multiple components jointly, while not being contained by any individual source?

Although there is a long tradition investigating such questions, a general formal framework to address them was developed only in 2010 in the form of *Partial Information Decomposition* (PID) [24]. When considering  $n = 2$  sources, the total information about  $Y$  given by  $X_1$  and  $X_2$  is decomposed as

$$I(X_1, X_2 : Y) = \Pi(\{1\}, \{2\}) + \Pi(\{1, 2\}) + \sum_{i=1}^2 \Pi(\{i\}), \quad (\text{A2})$$

where the four resulting components — known as ‘information atoms’ — can be described as:

- *Unique information*: information about  $Y$  uniquely contained in  $X_i$ , denoted by  $\Pi(\{i\})$ ,  $i \in \{1, 2\}$ .

- *Redundant information*: information about  $Y$  redundantly contained in both  $X_1$  and  $X_2$ , denoted by  $\Pi(\{1\}\{2\})$ .
- *Synergistic information*: information about  $Y$  synergistically contained in  $X_1$  and  $X_2$  jointly but not contained in either of them individually, denoted by  $\Pi(\{1, 2\})$ .

Furthermore, considering the well-known chain rule of the mutual information, which states that  $I(X_1, X_2 : Y) = I(X_1 : Y) + I(X_2 : Y|X_1)$ , it is natural to demand the following relationships:

$$I(X_1 : Y) = \Pi(\{1\}\{2\}) + \Pi(\{1\}), \quad (\text{A3})$$

$$I(X_2 : Y) = \Pi(\{1\}\{2\}) + \Pi(\{2\}), \quad (\text{A4})$$

$$I(X_1 : Y|X_2) = \Pi(\{1, 2\}) + \Pi(\{1\}), \quad (\text{A5})$$

$$I(X_2 : Y|X_1) = \Pi(\{1, 2\}) + \Pi(\{2\}). \quad (\text{A6})$$

Thus, the joint mutual information is made up of the sum of all four atoms; the marginal mutual information consists of unique information plus redundancy; and the conditional mutual information consists of unique information plus synergy.

How does this decomposition generalise to a larger number of sources? A key principle for carrying out this extension is the idea of *containment* of information in different subsets of source variables [39], which we explain in the following. In the case of  $n = 2$  sources, there are three possible collections of (indices of) source variables:  $\{1\}$ ,  $\{2\}$ , and  $\{1, 2\}$ . Every possible type of information containment among those variables can be expressed as a table of binary encodings, where the columns correspond to possible collections of source variables and the rows contain zeros and ones describing containment or non-containment of information. Table II shows this construction for  $n = 2$ .

Type	$\{1\}$	$\{2\}$	$\{1, 2\}$
Unique to $X_1$	1	0	1
Unique to $X_2$	0	1	1
Redundancy	1	1	1
Synergy	0	0	1

TABLE II. Information containment in subsets of source variables for  $n = 2$  leading to four information atoms.

As explained in Ref. [39], these are all the possible containment relationships that satisfy some minimal requirements — namely, that assignment of 0’s and 1’s are monotonic with respect to inclusion (e.g., if some information is contained in  $I(X_1 : Y)$ , it must also be contained in  $I(X_1, X_2 : Y)$ ), and that the collection of all sources should always be assigned a 1. Building on these ideas, one can decompose the information given by  $n$  source variables by accounting for all possible ways in which information can be contained within subsets of sources. Each such pattern of containment corresponds

to a row in the associated containment table, and defines a distinct information atom (for more details, see Ref. [39]).

We can refer to an atom more concisely (i.e. without writing its corresponding row in the table) via the sets  $\mathbf{a}_1, \dots, \mathbf{a}_m \subseteq [n]$  it is contained in, leaving it implicit that it is not contained in any other set. In fact, due to monotonicity it is sufficient to refer to an atom via the *smallest sets that it is contained in* (with respect to the subset relation). It is then left implicit that it is also contained in any superset of those sets. This is the standard notation used in the PID literature and the one we have been using throughout this paper. For example, the information unique to  $X_1$  is  $\Pi(\{1\})$  since  $\{1\}$  is the smallest set of source variables that this information is contained in. By monotonicity, it is understood that it must also be in any superset of it, namely  $\{1, 2\}$ . And it is also understood that it is not contained in  $\{2\}$ .

So in general, given subsets of source variables  $\mathbf{a}_1, \dots, \mathbf{a}_m \subseteq [n]$ , the atom  $\Pi(\mathbf{a}_1, \dots, \mathbf{a}_m)$  is understood as the information contained exactly in all  $I(\mathbf{a}_i : Y)$ , and by monotonicity also in any sets that are supersets of some  $\mathbf{a}_i$ , but not contained anywhere else. Note that because of monotonicity, the domain of  $\Pi$  reduces to the so called *antichains* of the partial order  $([n], \subseteq)$ , i.e. sets  $\mathbf{a}_1, \dots, \mathbf{a}_m$  such that no set is a superset of another set. For instance, the meaning of  $\Pi(\{1\})$  and  $\Pi(\{1\}\{1, 2\})$  would be exactly the same. Hence, we can remove  $\{1, 2\}$  and only refer to the atom by the smallest set it is contained in. We refer to antichains of source variables by greek letters  $\alpha, \beta$ , etc. and denote the corresponding atoms by  $\Pi(\alpha), \Pi(\beta)$ , etc.

This construction of a decomposition where the components (atoms) are defined by their specific containment relations immediately suggests a quantitative relationship between the atoms and the different mutual information terms  $I(\mathbf{a} : Y)$ . Any such mutual information should be the sum of atoms that are contained in it. These are exactly the ones associated with antichains containing some subset of  $\mathbf{a}$  as an element

$$I(\mathbf{a}; Y) = \sum_{\exists \mathbf{b} \subseteq \mathbf{a} : \mathbf{b} \in \alpha} \Pi(\alpha) \quad (\text{A7})$$

This is the basic *consistency equation* of PID. We will adopt as a minimal notion of a PID any set of quantities  $\Pi(\alpha)$  that satisfy A7. There is a considerable literature on additional properties one might demand of a PID. We will indicate where such additional properties come into play when necessary, but for the most part the results presented in this paper only depend on A7. Note that due to the chain rule for mutual information the consistency equation can also be written in terms of conditional mutual information as

$$I(\mathbf{a}^C; Y | \mathbf{a}) = \sum_{\neg \exists \mathbf{b} \subseteq \mathbf{a} : \mathbf{b} \in \alpha} \Pi(\alpha) \quad (\text{A8})$$

which is obtained by subtracting the joint mutual information from both sides of A7 and multiplying them by

minus one.

One important fact about PID atoms is that they have a natural order in terms of their accessibility, i.e. we can say that an atom  $\Pi(\alpha)$  is "lower" than  $\Pi(\beta)$  just in case  $\Pi(\beta)$  is accessible via all sets of source variables via which  $\Pi(\alpha)$  is accessible. More formally, this means that whenever there is a 1 in the row of the containment table corresponding to  $\Pi(\beta)$  there must also be a 1 in the row corresponding to  $\Pi(\alpha)$ . In terms of the antichains  $\alpha, \beta$  this order can be shown to be given by

$$\alpha \preceq \beta \Leftrightarrow \forall \mathbf{b} \in \beta \exists \mathbf{a} \in \alpha : \mathbf{b} \supseteq \mathbf{a} \quad (\text{A9})$$

Intuitively, if all the sets of sources from which we obtain  $\Pi(\beta)$  enclose a set from which we obtain  $\Pi(\alpha)$ , then if  $\Pi(\beta)$  is accessible  $\Pi(\alpha)$  must be accessible as well. The set of antichains  $\mathcal{A}$  equipped with the partial order  $\preceq$  forms a lattice conventionally called the *redundancy lattice* in the PID literature [24].

Within the approach adopted here, the terminology of the "redundancy lattice" can be understood as follows. If we take a particular antichain  $\alpha = \{\mathbf{a}_1, \dots, \mathbf{a}_m\}$  and sum all PID atoms downwards on the lattice, we recover a notion of redundant information, denoted  $I_{\cap}(\alpha; Y)$ , that the source collections  $\mathbf{a}_1, \dots, \mathbf{a}_m$  jointly provide about the target variable  $T$ :

$$I_{\cap}(\alpha; Y) = \sum_{\beta \preceq \alpha} \Pi(\beta). \quad (\text{A10})$$

This construction precisely captures all those atoms contained in *every* mutual information term  $I(\mathbf{a}_i; Y)$ , hence capturing their redundancy. Consequently, redundancy terms corresponding to lower antichains in the lattice are fully included within redundancy terms corresponding to higher antichains. In this way, the redundancy lattice expresses the nested, hierarchical structure of redundant information.

Figure 4 illustrates the lattice  $(\mathcal{A}, \preceq)$  for  $n = 3$ . The all-way redundancy between all three sources appears at the very bottom of the lattice because it is the most accessible information atom. The all-way synergy atom appears at the very top of the lattice since it is the least accessible information atom.

Note the contrast to the original exposition of PID theory [24], which begins with an analysis of redundant information and subsequently defines the information atoms implicitly. In contrast, the approach taken here introduces the PID atoms directly as fundamental quantities. This atom-focused perspective is particularly suited to the objectives of this paper since our analysis exclusively relies on structural relationships between atoms and mutual information and conditional mutual information as specified in equations (A7) and (A8). Consequently, explicit reference to an underlying redundancy function becomes unnecessary. For further details on the relationship between the atom-focused perspective and the conventional PID framework, see [37].



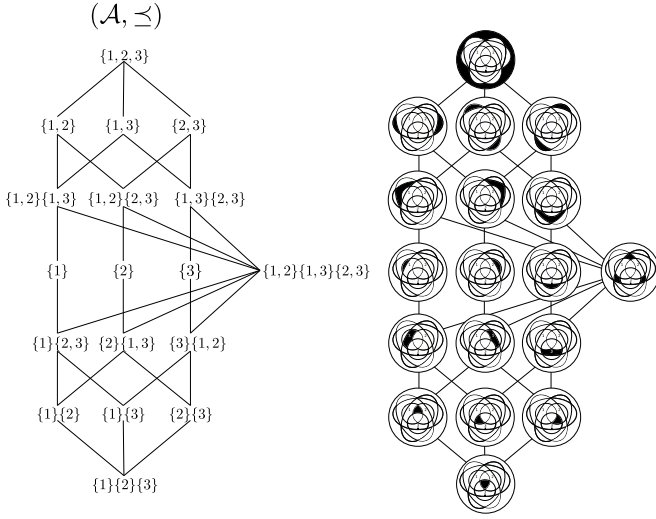


FIG. 4. Lattice of PID atoms for  $n = 3$  source variables (left). Corresponding representation of PID atoms in information diagrams (right).

## Appendix B: Bounds on information atoms derived from summary measures

For the interpretation of the degrees of redundancy and vulnerability in PID terms it is important to understand the bounds placed by certain values of  $\bar{r}$  and  $\bar{v}$  on different kinds information atoms. We have the following proposition (for the definitions of  $I_r^{(k)}$  and  $I_v^{(k)}$  see IID):

**Proposition 5.** *Assuming non-negativity of PID atoms,  $\frac{I_r^{(0)}}{I(\mathbf{X};Y)} \geq 1 - \bar{r}$  and  $\frac{I_v^{(0)}}{I(\mathbf{X};Y)} \geq 1 - \bar{v}$ .*

*Proof.* We argue the case for  $\bar{r}$ . The argument for  $\bar{v}$  is analogous. First, the normalized k-redundancies must sum up to 1:

$$\sum_{k=0}^n \frac{I_r^{(k)}}{I(\mathbf{X};Y)} = 1 \quad (\text{B1})$$

Thus,

$$\frac{I_r^{(0)}}{I(\mathbf{X};Y)} = 1 - \left( \sum_{k=1}^n \frac{I_r^{(k)}}{I(\mathbf{X};Y)} \right) \quad (\text{B2})$$

$$\geq 1 - \left( \sum_{k=1}^n k \frac{I_r^{(k)}}{I(\mathbf{X};Y)} \right) = 1 - \bar{r} \quad (\text{B3})$$

□

Note that for  $\bar{r} > 1$  or  $\bar{v} > 1$  the statement is true but trivial because assuming non-negativity of atoms already implies that  $I_r^{(0)}$  and  $I_v^{(0)}$  must be non-negative.

**Corollary 3.** *As special cases the proposition implies*

1.  $\bar{r} < 1$  means that there must be some source-level synergy, i.e.  $I_r^{(0)} > 0$ .

2.  $\bar{r} < 0.5$  means that source-level synergy is predominant, i.e.  $\frac{I_r^{(0)}}{I(\mathbf{X};Y)} > 0.5$ .
3.  $\bar{v} < 1$  means that there must be some robustness, i.e.  $I_v^{(0)} > 0$ .
4.  $\bar{v} < 0.5$  means that robustness is predominant, i.e.  $\frac{I_v^{(0)}}{I(\mathbf{X};Y)} > 0.5$ .

The interpretation of values of  $\bar{r}$  and  $\bar{v}$  larger than one is slightly more complicated, as it involves the components of these measures that distinguish between different orders of redundancy and vulnerability—where higher-order terms are weighted more heavily. Thus, values larger than one can always be explained in two distinct ways: either by a large weight on lower-order terms or by a smaller weight on higher-order terms. Hence, in general the bounds on redundancy and vulnerability to be inferred from such values depend on  $n$  since this determines how many orders of redundancy or vulnerability are distinguished. We have the following proposition for these bounds:

**Proposition 6.** *Assuming non-negativity of information atoms,*

$$\frac{\sum_{k=2}^n I_r^{(k)}}{I(\mathbf{X};Y)} \geq \frac{\bar{r} - 1}{n - 1} \quad (\text{B4})$$

and

$$\frac{\sum_{k=2}^n I_v^{(k)}}{I(\mathbf{X};Y)} \geq \frac{\bar{v} - 1}{n - 1} \quad (\text{B5})$$

*Proof.* Again we argue the case  $\bar{r}$  with the argument for  $\bar{v}$  proceeding in the same way. For any given value of  $\bar{r} > 1$  the scenario requiring the least proportion of redundancy is the one where all redundancy is of the highest-order and there is no source-level synergy. In this case, we have

$$\bar{r} = \frac{I_r^{(1)}}{I(\mathbf{X};Y)} + n \frac{I_r^{(n)}}{I(\mathbf{X};Y)} \quad (\text{B6})$$

$$= \left( 1 - \frac{I_r^{(n)}}{I(\mathbf{X};Y)} \right) + n \frac{I_r^{(n)}}{I(\mathbf{X};Y)} \quad (\text{B7})$$

$$= (n - 1) \frac{I_r^{(n)}}{I(\mathbf{X};Y)} + 1 \quad (\text{B8})$$

which implies

$$\frac{\bar{r} - 1}{n - 1} = \frac{I_r^{(n)}}{I(\mathbf{X};Y)} \quad (\text{B9})$$

This is therefore the minimal value required to achieve the given value of  $\bar{r}$ . □

**Corollary 4.** *The proposition entails in particular that*

1.  $\bar{r} > 1$  means that there must be some proper redundancy, i.e.  $I_r^{(k)} > 0$  for some  $k > 1$ .



2.  $\bar{r} > \frac{1}{2}(n+1)$  means that redundancy is predominant, i.e.  $\frac{\sum_{k=2}^n I_r^{(k)}}{I(\mathbf{X};\mathbf{Y})} > 0.5$ .
3.  $\bar{v} > 1$  means that there must be some vulnerability of degree larger one, i.e.  $I_v^{(k)} > 0$  for some  $k > 1$ .
4.  $\bar{v} > \frac{1}{2}(n+1)$  means that vulnerability of degree larger one is predominant, i.e.  $\frac{\sum_{k=1}^n I_v^{(k)}}{I(\mathbf{X};\mathbf{Y})} > 0.5$ .

In 2. and 4. we can see the dependence on  $n$ : the larger  $n$  the higher the values necessary to infer a predominance of redundancy or vulnerability. A more general statement regarding the required values to infer a certain percentage of redundancy or vulnerability is

**Corollary 5.**

$$\frac{\sum_{k=1}^n I_r^{(k)}}{I(\mathbf{X};\mathbf{Y})} > \lambda \Leftrightarrow \bar{r} > \lambda(n + \frac{1-\lambda}{\lambda}) \quad (\text{B10})$$

$$\frac{\sum_{k=1}^n I_v^{(k)}}{I(\mathbf{X};\mathbf{Y})} > \lambda \Leftrightarrow \bar{v} > \lambda(n + \frac{1-\lambda}{\lambda}) \quad (\text{B11})$$

### Appendix C: Neural Network Implementation Details

The neural networks in this work have been implemented using the “nninfo” python package for information-theoretic analysis of deep neural networks (<https://github.com/Priesemann-Group/nninfo>, [27]) which builds on the pytorch framework.

To achieve finite and non-trivial information dynamics, the activations of all neurons have been quantized stochastically to one of the two nearest of eight quantization levels between the bounds of the activation function  $\sigma_{\min}$  and  $\sigma_{\max}$  with equal distances  $\epsilon = (\sigma_{\max} - \sigma_{\min})/(n_{\text{levels}} - 1)$ . The rounded activation values  $\ell$  are obtained from the raw activation values  $\hat{\ell}$  as

$$\ell = \epsilon\lambda + \sigma_{\min}$$

where

$$\lambda = \begin{cases} \left\lceil \frac{\hat{\ell} - \sigma_{\min}}{\epsilon} \right\rceil & r > \left( \frac{\hat{\ell} - \sigma_{\min}}{\epsilon} \bmod 1 \right) \\ \left\lfloor \frac{\hat{\ell} - \sigma_{\min}}{\epsilon} \right\rfloor & r \leq \left( \frac{\hat{\ell} - \sigma_{\min}}{\epsilon} \bmod 1 \right), \end{cases}$$

Here,  $r \in [0, 1]$  is drawn i.i.d. from a uniform distribution for each neuron and each evaluation.

The *MNIST classifier network* is a fully-connected feed-forward deep neural network using a one-hot output representation and tanh activation functions. The networks were trained 10 times for  $10^4$  epochs with different Xavier random weight initializations, using cross entropy loss and a constant SGD learning rate of 0.01.

$n_b$	Final train loss	Final test loss
128	$9.43(9) \times 10^{-3}$	$9.5(1) \times 10^{-3}$
20	$1.70(4) \times 10^{-2}$	$1.70(4) \times 10^{-2}$
16	$1.86(3) \times 10^{-2}$	$1.86(3) \times 10^{-2}$
12	$2.12(4) \times 10^{-2}$	$2.12(4) \times 10^{-2}$

TABLE III. Final train and test set mean square error losses for the face autoencoder network for different bottleneck sizes  $n_b$ .

They achieve a final train set accuracy of 99.89(3)% and a test set accuracy of 95.5(3)%.

For the *Face autoencoder network*, the “Labelled faces in the Wild”[61] dataset is augmented by adding images that have been flipped horizontally as well as rotated by  $-10, -5, 0, 5$  or  $10$  degrees. Combining these augmentations, the dataset is expanded to ten times more samples which have similar statistics as the original images, which enables the estimation of small information-theoretic quantities. The images are preprocessed by resizing the original images to  $40 \times 40$  pixels before cropping 4 pixels from each border to produce  $32 \times 32$  images with three color channels.

The network has three convolutional encoder layers with a kernel size of  $3 \times 3$ , padding of 1 and  $2 \times 2$  max pooling layers after each. The output of the third convolutional layer is linearized and fully connected to a variable-size bottleneck layer, after which three transpose convolutional layers with kernel size 3 and stride of 2 finally produce a reconstruction of the input image. As in the MNIST example, all layers use tanh activation functions. The autoencoder networks use mean square error and the Adam optimizer with an initial learning rate of 0.001. The autoencoder networks were run 10 times each for  $n_b = 128$ ,  $n_b = 20$ ,  $n_b = 16$  and  $n_b = 12$  neurons in the bottleneck layer each with different Xavier weight initializations. The final train and test set losses after  $10^3$  epochs are summarized in Table III.

[1] M. M. Waldrop, *Complexity: The emerging science at the edge of order and chaos* (Simon and Schuster, 1993).

[2] J. Gleick, *The information: A history, a theory, a flood* (Vintage, 2011).

- [3] Y. Bengio and N. Malkin, Bulletin of the American Mathematical Society **61**, 457 (2024).
- [4] H. Rajpal, C. von Stengel, P. A. Mediano, F. E. Rosas, E. Viegas, P. A. Marquet, and H. J. Jensen, arXiv preprint arXiv:2310.20386 (2023).
- [5] Z. Cang and Q. Nie, Nature Communications **11**, 2084 (2020).
- [6] S. Park, F. Supek, and B. Lehner, Nature communications **12**, 7051 (2021).
- [7] D. Marinazzo, J. Van Roozendaal, F. E. Rosas, M. Stella, R. Comolatti, N. Colenbier, S. Stramaglia, and Y. Rosseel, arXiv preprint arXiv:2205.01035 (2022).
- [8] T. F. Varley and P. Kaminski, Entropy **24**, 1387 (2022).
- [9] F. Rosas, P. A. Mediano, M. Ugarte, and H. J. Jensen, Entropy **20**, 793 (2018).
- [10] P. Orio, P. A. Mediano, and F. E. Rosas, Chaos: An Interdisciplinary Journal of Nonlinear Science **33** (2023).
- [11] T. Scagliarini, D. Marinazzo, Y. Guo, S. Stramaglia, and F. E. Rosas, Physical Review Research **4**, 013184 (2022).
- [12] M. Gatica, R. Cofré, P. A. Mediano, F. E. Rosas, P. Orio, I. Diez, S. P. Swinnen, and J. M. Cortes, Brain Connectivity **11**, 734 (2021).
- [13] A. I. Luppi, P. A. Mediano, F. E. Rosas, N. Holland, T. D. Fryer, J. T. O'Brien, J. B. Rowe, D. K. Menon, D. Bor, and E. A. Stamatakis, Nature Neuroscience **25**, 771 (2022).
- [14] T. F. Varley, O. Sporns, S. Schaffelhofer, H. Scherberger, and B. Dann, Proceedings of the National Academy of Sciences **120**, e2207677120 (2023).
- [15] T. F. Varley, M. Pope, J. Faskowitz, and O. Sporns, Communications Biology **6**, 451 (2023).
- [16] R. Herzog, F. M. Barbey, M. N. Islam, L. Rueda-Delgado, H. Nolan, P. Prado, M. Krylova, I. Izyurov, N. Javaheripour, L. V. Danyeli, *et al.*, Translational Psychiatry **14**, 310 (2024).
- [17] M. Pope, T. F. Varley, and O. Sporns, bioRxiv, 2024 (2024).
- [18] T. F. Varley, O. Sporns, N. J. Stevenson, M. G. Welch, M. M. Myers, S. Vanhatalo, and A. Tokariev, bioRxiv, 2024 (2024).
- [19] T. M. Tax, P. A. Mediano, and M. Shanahan, Entropy **19**, 474 (2017).
- [20] A. M. Proca, F. E. Rosas, A. I. Luppi, D. Bor, M. Crosby, and P. A. Mediano, arXiv preprint arXiv:2210.02996 (2022).
- [21] C. Kaplanis, P. Mediano, and F. Rosas, in *NeurIPS 2023 workshop: Information-Theoretic Principles in Cognitive Systems* (2023).
- [22] X. Kong, O. Liu, H. Li, D. Yogatama, and G. V. Steeg, arXiv preprint arXiv:2310.07972 (2023).
- [23] A. I. Luppi, F. E. Rosas, P. A. Mediano, D. K. Menon, and E. A. Stamatakis, Trends in Cognitive Sciences (2024).
- [24] P. L. Williams and R. D. Beer, arXiv preprint arXiv:1004.2515 (2010).
- [25] J. T. Lizier, N. Bertschinger, J. Jost, and M. Wibral, "Information decomposition of target effects from multi-source interactions: Perspectives on previous, current and future work," (2018).
- [26] P. A. Mediano, F. E. Rosas, A. I. Luppi, R. L. Carhart-Harris, D. Bor, A. K. Seth, and A. B. Barrett, arXiv preprint arXiv:2109.13186 (2021).
- [27] D. A. Ehrlich, A. C. Schneider, V. Priesemann, M. Wibral, and A. Makkeh, *Transactions on Machine Learning Research* (2023).
- [28] A. C. Schneider, V. Neuhaus, D. A. Ehrlich, A. Makkeh, A. S. Ecker, V. Priesemann, and M. Wibral, in *Proc. 13th Int. Conf. on Learning Representations (ICLR)* (2025) <https://openreview.net/forum?id=CLE09ESvul>.
- [29] A. Makkeh, M. Graetz, A. C. Schneider, D. A. Ehrlich, V. Priesemann, and M. Wibral, *Proceedings of the National Academy of Sciences* **122**, e2408125122 (2025).
- [30] M. Wibral, V. Priesemann, J. W. Kay, J. T. Lizier, and W. A. Phillips, Brain and cognition **112**, 25 (2017).
- [31] T. F. Varley and J. Bongard, Chaos: An Interdisciplinary Journal of Nonlinear Science **34** (2024).
- [32] F. E. Rosas, P. A. Mediano, B. Rassouli, and A. B. Barrett, Journal of Physics A: Mathematical and Theoretical **53**, 485001 (2020).
- [33] C. Finn and J. Lizier, Entropy **20**, 297 (2018).
- [34] A. Makkeh, A. J. Gutknecht, and M. Wibral, Physical Review E **103**, 032149 (2021).
- [35] A. Kolchinsky, Entropy **24**, 403 (2022).
- [36] S. J. van Enk, Physical Review E **107**, 054133 (2023).
- [37] A. J. Gutknecht, A. Makkeh, and M. Wibral, *Proceedings of the Royal Society A* **481**, 20240174 (2025).
- [38] A. Jansma, P. A. Mediano, and F. E. Rosas, arXiv preprint arXiv:2410.06224 (2024).
- [39] A. J. Gutknecht, M. Wibral, and A. Makkeh, *Proceedings of the Royal Society A: Mathematical, Physical and Engineering Sciences* **477**, 20210110 (2021).
- [40] E. T. Jaynes, Physical review **106**, 620 (1957).
- [41] F. E. Rosas, B. C. Geiger, A. I. Luppi, A. K. Seth, D. Polani, M. Gastpar, and P. A. Mediano, arXiv preprint arXiv:2402.09090 (2024).
- [42] G. Chechik, A. Globerson, M. Anderson, E. Young, I. Nelken, and N. Tishby, in *Advances in Neural Information Processing Systems 14*, edited by T. G. Dietterich, S. Becker, and Z. Ghahramani (MIT Press, Cambridge, MA, 2002).
- [43] N. Timme, W. Alford, B. Flecker, and J. M. Beggs, Journal of Computational Neuroscience **36**, 119 (2014).
- [44] F. E. Rosas, P. A. M. Mediano, and M. Gastpar, arXiv preprint arXiv:2404.07140 (2024), <http://arxiv.org/abs/2404.07140>.
- [45] T. M. Cover, *Elements of information theory* (John Wiley & Sons, 1999).
- [46] R. G. James and J. P. Crutchfield, Entropy **19**, 531 (2017).
- [47] W. McGill, Transactions of the IRE Professional Group on Information Theory **4**, 93 (1954).
- [48] T. F. Varley and E. Hoel, Philosophical Transactions of the Royal Society A **380**, 20210150 (2022).
- [49] G. Chechik, A. Globerson, M. Anderson, E. Young, I. Nelken, and N. Tishby, in *Advances in Neural Information Processing Systems 14*, edited by T. G. Dietterich, S. Becker, and Z. Ghahramani (MIT Press, Cambridge, MA, 2002).
- [50] N. Brenner, S. P. Strong, R. Koberle, W. Bialek, and R. R. d. R. v. Steveninck, Neural computation **12**, 1531 (2000).
- [51] T. J. Gawne and B. J. Richmond, Journal of Neuroscience **13**, 2758 (1993).
- [52] V. Griffith and C. Koch, in *Guided self-organization: inception* (Springer, 2014) pp. 159–190.
- [53] S. Yang and J. Gu, Journal of Zhejiang University-Science A **5**, 1382 (2004).
- [54] I. Mares, C. Mares, V. Dobrica, and C. Demetrescu,

- Entropy **24**, 1375 (2022).
- [55] I. Mares, V. Dobrica, C. Demetrescu, and C. Mares, *Atmosphere* **14**, 1622 (2023).
  - [56] S. Luecke, X. Guo, K. M. Sheu, A. Singh, S. C. Lowe, M. Han, J. Diaz, F. Lopes, R. Wollman, and A. Hoffmann, *Molecular Systems Biology* **20**, 898 (2024).
  - [57] A. M. Saxe, Y. Bansal, J. Dapello, M. Advani, A. Kolchinsky, B. D. Tracey, and D. D. Cox, *Journal of Statistical Mechanics: Theory and Experiment* **2019**, 124020 (2019).
  - [58] Z. Goldfeld, E. v. d. Berg, K. Greenewald, I. Melnyk, N. Nguyen, B. Kingsbury, and Y. Polyanskiy, *International Conference on Machine Learning* (2019).
  - [59] B. C. Geiger, *IEEE Transactions on Neural Networks and Learning Systems* (2021).
  - [60] Y. LeCun, L. Bottou, Y. Bengio, and P. Haffner, *Proceedings of the IEEE* **86**, 2278 (1998).
  - [61] G. B. Huang, M. Ramesh, T. Berg, and E. Learned-Miller, *Labeled Faces in the Wild: A Database for Studying Face Recognition in Unconstrained Environments*, Tech. Rep. 07-49 (University of Massachusetts, Amherst, 2007).
  - [62] L. Belloli, P. Mediano, R. Cofré, D. F. Slezak, and R. Herzog, *arXiv preprint arXiv:2501.03381* (2025).
  - [63] P. Venkatesh, C. Bennett, S. Gale, T. Ramirez, G. Heller, S. Durand, S. Olsen, and S. Mihalas, *Advances in Neural Information Processing Systems* **36**, 74602 (2023).
  - [64] A. Liardi, F. E. Rosas, R. L. Carhart-Harris, G. Blackburne, D. Bor, and P. A. Mediano, *arXiv preprint arXiv:2410.11583* (2024).